

Co-infecting microorganisms dramatically alter pathogen gene essentiality during polymicrobial infection

Carolyn B. Ibberson¹, Apollo Stacy¹, Derek Fleming², Justine L. Dees¹, Kendra Rumbaugh², Michael S. Gilmore³ and Marvin Whiteley^{1*}

Identifying genes required by pathogens during infection is critical for antimicrobial development. Here, we use a Monte Carlo simulation-based method to analyse high-throughput transposon sequencing data to determine the role of infection site and co-infecting microorganisms on the *in vivo* 'essential' genome of *Staphylococcus aureus*. We discovered that co-infection of murine surgical wounds with *Pseudomonas aeruginosa* results in conversion of ~25% of the *in vivo* *S. aureus* mono-culture essential genes to non-essential. Furthermore, 182 *S. aureus* genes are uniquely essential during co-infection. These 'community dependent essential' (CoDE) genes illustrate the importance of studying pathogen gene essentiality in polymicrobial communities.

To cause infection, bacteria must possess the genetic requirements to colonize and proliferate within a host. These genes can be classified into two primary categories, those that are essential during all growth conditions (*in vitro* and *in vivo*) and those that are solely essential in the infection site (*in vivo*). Identification of essential genes is important for developing new therapeutics against human pathogens¹. Although most antimicrobials target factors essential under all growth conditions, there is increasing interest in targeting genes that are essential solely during infection^{2–4}.

The advent of high-throughput sequencing technologies greatly enhanced essential gene discovery both *in vitro* and *in vivo*. One such technology, transposon insertion site sequencing (Tn-seq), allows simultaneous assessment of the relative frequencies of tens of thousands of individual mutants following growth in specific environments⁵. This technique has allowed our laboratory and others to determine the essential genomes of microorganisms both *in vitro* and during infection^{3,6–8}. However, these studies have focused on mono-culture infections in single infection sites^{3,5–8}, despite the fact that many bacterial pathogens cause disease in multiple tissue types and often as part of diverse, multi-species communities⁹. In this study, we set out to determine the role of both infection site and co-infecting microorganisms on the *in vivo* essential genome of the pathogenic bacterium *Staphylococcus aureus*.

S. aureus is an excellent bacterium for these studies because it is well-adapted to survival in humans, persistently colonizing 30% of the human population¹⁰ and capable of infecting nearly every tissue of the human body¹¹. Types of infections caused by *S. aureus* range from primarily mono-species infections, such as skin and soft-tissue abscesses^{11,12}, to polymicrobial infections such as chronic wounds, where, on average, six species are isolated from an infection¹³.

S. aureus is the most common organism isolated from chronic wounds and is frequently found with the opportunistic pathogenic bacterium *Pseudomonas aeruginosa*¹³. Notably, chronic wounds harbouring both *S. aureus* and *P. aeruginosa* are associated with increased wound severity and increased healthcare costs^{13,14}.

Here, we have used Tn-seq and a Monte Carlo-based analysis to determine what we refer to as the 'essential genome' of *S. aureus* in three murine infection models and during co-infection with *P. aeruginosa*. Our results reveal that co-infection has a larger effect on the *S. aureus* essential genome than infection site, with ~200 genes showing altered essentiality during co-infection. A similar number of community dependent essential (CoDE) genes were also found in a periodontal pathogen using an unrelated polymicrobial infection model. Collectively, this work illustrates the importance of studying pathogens in complex polymicrobial communities.

Results and discussion

We first used a Monte Carlo-based analysis^{3,15} of a transposon mutant pool containing ~72,000 insertions⁷ in *S. aureus* strain HG003 to determine the *in vitro* *S. aureus* essential genome in rich laboratory media. Briefly, this analysis compares transposon abundances in the library (observed data set) to an expected data set where transposons are randomly redistributed *in silico* across the genome (see Methods). For this study, 'essential genes' are defined as genes that, in a condition, (1) have a reduced fold change in the insertion frequency compared to the expected data set and (2) cluster with the lower mode in the characteristic¹⁶ bimodal distribution of fold changes comparing the observed and expected data sets. This analysis identified 512 *S. aureus* genes that are essential for *S. aureus* growth *in vitro* (Supplementary Table 1). As expected, these genes are enriched for central cellular processes, including central metabolism and ribosome activity (Fisher's exact test *P* value of <0.05).

We then used a Monte Carlo approach to investigate how infection site affects the *S. aureus* essential genome during mono-culture infection. We analysed previously generated Tn-seq data from murine abscess⁷ and osteomyelitis⁸ models, as well as data generated in this study from a murine chronic surgical wound model. This latter model is well established for studying polymicrobial *S. aureus* wound infections and requires over a week for resolution^{17,18}. To specifically focus on the *in vivo* essential genome, we removed the 512 *in vitro* essential genes from all subsequent analyses. We identified 280 genes that are essential in at least one infection model (Fig. 1a), but not *in vitro*. Of these genes, 39 (14%) were essential in all

¹Department of Molecular Biosciences, Institute for Cellular and Molecular Biology, LaMontagne Center for Infectious Disease, The University of Texas at Austin, 1 University Station, A5000, Austin, Texas 78712, USA. ²Department of Surgery, Texas Tech University Health Sciences Center, Lubbock, Texas 79430, USA. ³Department of Ophthalmology and Department of Microbiology and Immunobiology, Harvard Medical School, Massachusetts Eye and Ear Infirmary, Boston, Massachusetts 02115, USA. *e-mail: mwhiteley@austin.utexas.edu

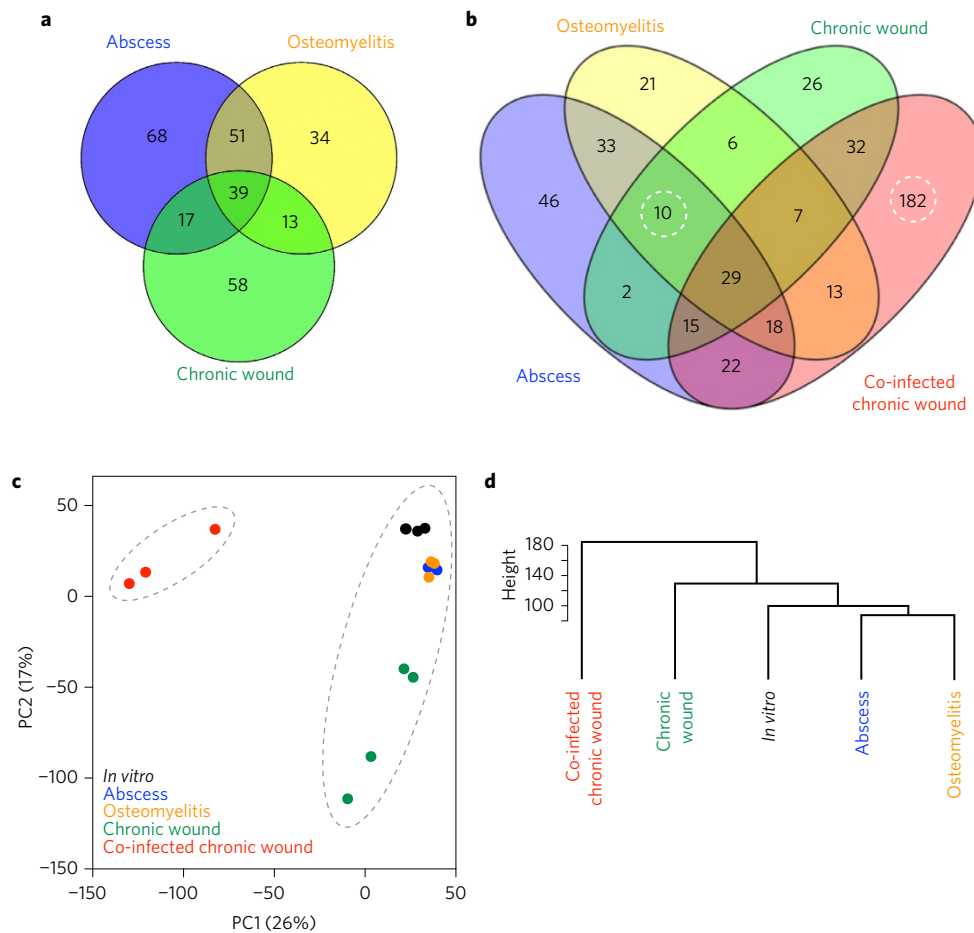


Figure 1 | The *S. aureus* *in vivo* essential genome in three monoculture infections and during co-infection with *P. aeruginosa*. **a**, Venn diagram of the *S. aureus* *in vivo* essential genome in mono-culture murine abscess (blue, $n = 2$), osteomyelitis (yellow, $n = 3$) and chronic surgical wound (green, $n = 4$) models of infection. **b**, Venn diagram of the *S. aureus* *in vivo* essential genome during abscess (blue), osteomyelitis (yellow), chronic surgical wound mono-culture infection (green) and chronic surgical wound co-culture infection with *P. aeruginosa* (red). Dashed circles highlight the 10 *S. aureus* CoDE genes that were essential in all mono-culture infections but non-essential in co-culture, and the 182 *S. aureus* CoDE genes that were unique to co-infection in the chronic surgical wound. False positive rates for the essential gene analysis were determined as outlined in the Methods ('Essential gene analysis') and yielded 0 genes for abscess, 4 genes for osteomyelitis, 1 gene for mono-infection chronic surgical wound and 18 genes for co-infection chronic surgical wound. **c**, Plot of the first two principal components (PCs) generated by PCA of the normalized read counts per *S. aureus* gene in five conditions: *in vitro* BHI growth⁷ (black, $n = 4$, only three points are distinguishable due to overlap), murine abscess (blue, $n = 2$), murine osteomyelitis (orange, $n = 3$), murine chronic surgical wound mono-infection (green, $n = 4$) and murine chronic surgical wound co-infection with *P. aeruginosa* (red, $n = 3$). Dashed grey circles indicate the two clusters that are generated by k-means clustering analysis. **d**, Hierarchical clustering (Ward method) of the average normalized counts per gene in each of the conditions described above. Height indicates the Euclidean distance between clusters. Similar clustering results were obtained with individual replicates (Supplementary Fig. 3).

three mono-infection models and 120 (43%) were essential in at least two models. However, 68 (24%) were unique to the abscess, 34 (12%) were unique to osteomyelitis and 58 (21%) were unique to the chronic surgical wound. These data indicate that infection site can have a substantial impact on the *in vivo* essential genome and that *S. aureus* possesses a core set of *in vivo* essential genes across all infection models.

Chronic wound infections are predominantly polymicrobial, with *S. aureus* and *P. aeruginosa* being the most commonly isolated microorganisms^{13,14,19,20}. Therefore, we next assessed how the presence of *P. aeruginosa* impacts the *S. aureus* *in vivo* essential genome in the murine chronic surgical wound model. For these experiments, tenfold less *P. aeruginosa* than *S. aureus* was used in the inoculum to ensure that the effects observed were not due to increased bacterial inoculum. We compared the *S. aureus* Tn-seq data generated in all four infections and *in vitro* through k-means clustering of the principal component analysis (PCA) and hierarchical clustering, and found that the chronic surgical wound co-infection data clustered independently from mono-culture infections by both

methods (Fig. 1c,d). These findings indicate the essential genome of *S. aureus* is distinct during co-infection compared to mono-infection.

Additional examination revealed that 182 genes, representing over 6% of the *S. aureus* genome, are uniquely essential to *S. aureus* during chronic surgical wound co-infection (Fig. 1b). Furthermore, these genes were significantly enriched (Fisher's exact test, $P < 0.05$) in the clusters of orthologous groups (COG) functional categories for energy production and conversion, as well as amino acid, nucleotide, carbohydrate, lipid and inorganic ion metabolism (Supplementary Table 1). These data suggest that *P. aeruginosa* induces a metabolic stress on *S. aureus* in the chronic surgical wound. Of note, these genes also included the global regulator repressor of toxins (*rot*, SAOUHSC_01879), a phenol-soluble modulins (*psmβ1*, SAOUHSC_01135) and multiple components of the *S. aureus* Type VII secretion system^{21,22} (SAOUHSC_00260, SAOUHSC_00264 and SAOUHSC_00265). In addition, we discovered ten genes, representing 26% of the genes essential in all three mono-infections, that were no longer essential

during co-infection with *P. aeruginosa* (Fig. 1b and Supplementary Table 1). These included genes coding for menaquinol oxidase (*goxC*, SAOUHSC_01000) and ATP synthase (*atpD*, SAOUHSC_02341). To ensure the accuracy of our population-scale Tn-seq analyses, we competed three individual transposon mutants (the mono-infection-specific essential gene mutant *yrrK*, the co-infection-specific essential gene mutant *udk* and mutant *vWbp* (a.k.a. *graB*) that did not change in abundance) against the wild-type strain in mono- and co-infection in the murine chronic surgical wound (Fig. 2a and Supplementary Table 7). In addition, we assessed a small pool of transposon mutants in a small-scale murine chronic surgical wound Tn-seq experiment (Fig. 2b). In all cases, these experiments confirmed the findings of the original genome-scale Tn-seq experiments. Together, these results indicate that the *S. aureus in vivo* essential genome is dramatically altered during co-infection with *P. aeruginosa* both through the emergence of essential genes (182 genes) and alleviation of the requirement for mono-culture essential genes (10 genes), which, in sum, we term ‘community dependent essential’ (CoDE) genes. The fact that the number of CoDE genes (192) is twice as large as the total number of genes unique to all mono-culture infection sites (93) suggests that the presence of a co-infecting bacterium impacts the *in vivo* essential genome more significantly than infection site.

An important question is whether *S. aureus* CoDE genes are restricted to the murine chronic surgical wound infection. To investigate this, we assessed the phenotypes of multiple CoDE gene mutants in an *in vitro* wound model²³. This well-characterized^{23,24} model allows *P. aeruginosa* and *S. aureus* to spatially segregate in a coagulated matrix and thus promotes synergistic interactions, such as enhanced resistance to antibiotics and formation of distinct aggregates²⁴. From our Tn-seq analysis (Supplementary Table 1), we predicted *graE*, *udk* and *tcyA* would be required in co-culture but not in mono-culture, and conversely, *yrrK* and *atpD* would be required in mono-culture but not co-culture. Surprisingly, four of the five *S. aureus* CoDE gene mutants showed the predicted phenotypes in the *in vitro* wound model (Supplementary Fig. 1), supporting the importance of CoDE genes for *S. aureus* fitness beyond the murine wound environment.

A remaining question is whether other pathogens exhibit a similarly high prevalence of CoDE genes during polymicrobial infection. Therefore, we tested for CoDE genes in the oral pathogenic bacterium *Aggregatibacter actinomycetemcomitans* during mono- and co-infection with the oral commensal bacterium *Streptococcus gordonii*. This model is useful for assessing CoDE genes, as *A. actinomycetemcomitans* and *S. gordonii* co-localize in the human oral cavity²⁵ and synergistically interact in a murine abscess infection model²⁶. As with *S. aureus*, genes that were essential *in vitro* were removed from our analysis to focus on *A. actinomycetemcomitans in vivo* essential genes (Supplementary Table 1). *A. actinomycetemcomitans* Tn-seq data from mono- and co-infected abscesses revealed that ~47% (155 genes) of its *in vivo* essential genome are CoDE genes (Supplementary Fig. 2). Similar to our findings with *S. aureus*, co-infection with *S. gordonii* places unique metabolic stresses on *A. actinomycetemcomitans* as multiple nutrient transporters and biosynthesis pathways were solely required during co-infection (Supplementary Table 1). Additionally, this analysis confirmed a previous observation that, while *A. actinomycetemcomitans* requires *atpB* in mono-infection, the presence of *S. gordonii* alleviates this requirement²⁷. Collectively, these data indicate that CoDE genes are not limited to *S. aureus/P. aeruginosa* wound infections.

For over 100 years, it has been recognized that many human infections are caused by microbial communities, not individual microorganisms. However, microbial pathogens are frequently studied in isolation in animal infection models. Our discovery of CoDE genes reveals it is critical to identify a pathogen’s essential

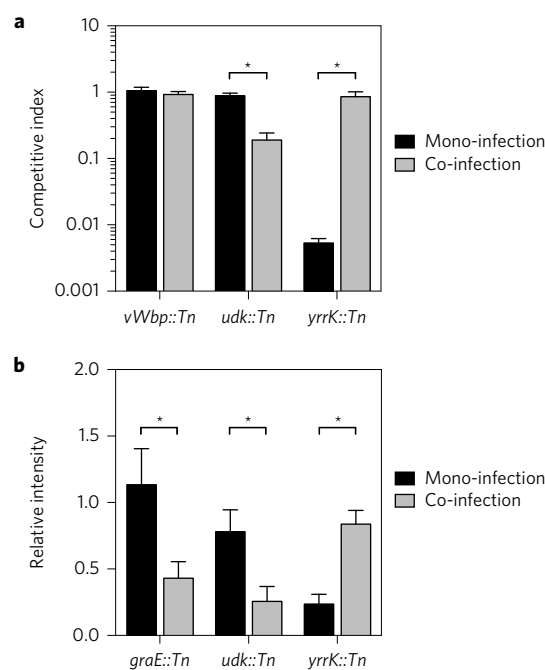


Figure 2 | Confirmation of *S. aureus* mutant Tn-seq phenotypes. **a**, Three *S. aureus* transposon mutants were competed with the wild-type *S. aureus* strain HG003 in mono- and co-infection with *P. aeruginosa* PAO1 in the murine chronic surgical wound. Mutations in the CoDE gene *udk::TnMariner* (SAOUHSC_01715) were predicted to be essential in co-infection but not mono-infection, while *yrrK::TnMariner* (SAOUHSC_01720) was predicted to be essential in mono-infection but not in co-infection. An *S. aureus* mutant whose relative abundance did not change (*vWbp::TnMariner*, SAOUHSC_00814) in the initial Tn-seq experiments (Supplementary Table 1) was used as a control. For each condition, three biological replicates were used. **b**, A subset of *S. aureus* transposon mutants were pooled and used to infect the murine chronic surgical wound alone and in co-infection with *P. aeruginosa* (three mice each). DNA was extracted four days post-infection, and PCR was used to quantify the relative abundance of each *S. aureus* mutant. As a control, an *S. aureus* mutant whose relative abundance did not change (*vWbp::TnMariner*, SAOUHSC_00814) in the initial Tn-seq experiments (Supplementary Table 1) was used for normalization. Mutations in the CoDE genes *graE::TnMariner* (SAOUHSC_01600) and *udk::TnMariner* were predicted to be essential in co-infection but not mono-infection, while *yrrK::TnMariner* was predicted to be essential in mono-infection but not in co-infection. The intensity of PCR amplicons was calculated using ImageJ (FIJI) and relative intensity was calculated by dividing CoDE gene amplicon intensity by *vWbp::TnMariner* amplicon intensity. Statistical analysis was performed using a Student’s *t*-test ($*P < 0.05$). Error bars represent the standard error of the mean (s.e.m.). Bars represent three biological replicates, and three technical replicates (total of nine replicates) for *udk::TnMariner* and *graE::TnMariner*, and three biological, two technical replicates (six total replicates) for *yrrK::TnMariner*. The average total number of *S. aureus* (\pm s.e.m.) recovered from mono-culture wounds was $3 \times 10^8 \pm 5 \times 10^7$ c.f.u. g^{-1} and from co-culture wounds was $6.0 \times 10^8 \pm 3 \times 10^7$ c.f.u. g^{-1} .

genes in complex communities that reflect native infections. This is particularly relevant when designing antimicrobials, because co-infection-specific genes could serve as new therapeutic targets for multi-species infections, while CoDE genes that are no longer essential in co-infection may only be effective targets in mono-culture infections. As with all essential gene analyses, there are limitations to these findings. Due to the nature of Tn-seq, mutants can cross-complement each other, so secreted factors are often not identified. Additionally, it is possible some mutations will not disrupt protein function or some genes may have few transposon

insertions, limitations we have addressed in our essential gene analysis (see Methods). Finally, it should be noted we have used a precise definition for ‘essential genes’ that may differ from other studies, although all CoDE genes can clearly be defined as *in vivo* fitness determinants. Overall, we believe these findings have broad implications for polymicrobial infections, and it will be interesting to explore the exact mechanisms by which the presence of co-infecting microorganisms leads to CoDE genes.

Methods

Ethics statement. This study was carried out in strict accordance with the recommendations in the Guide for the Care and Use of Laboratory Animals of the National Institutes of Health (NIH). Animal protocols were approved by the Institutional Animal Care and Use Committees of The University of Texas at Austin (protocol no. 00136) and Texas Tech University Health Sciences Center (protocol no. 07044).

Bacterial strains and culture conditions. Previously generated transposon mutant libraries of *S. aureus* strain HG003 (ref. 7) and *P. aeruginosa* strain PAO1 (ref. 28) were used in this study. *S. aureus in vitro* cultures were grown in brain–heart infusion broth (BHI) at 37 °C, with shaking at 225 r.p.m. and a flask-to-media volume ratio of 5:1. All of the transposon mutants used in this study were provided by the Network on Antimicrobial Resistance in *Staphylococcus aureus* (NARSA) and distributed by BEI Resources, the National Institute of Allergy and Infectious Diseases and NIH. Mutations were moved to the *S. aureus* HG003 strain background by transduction using staphylococcal phage Φ 11 (ref. 29) and confirmed by polymerase chain reaction (PCR). All primer sequences are listed in Supplementary Table 3. The strains of oral bacteria used were *A. actinomycetemcomitans* 624 (a clinical isolate) and *S. gordonii* Challis DL1.1 (ATCC 49818). *A. actinomycetemcomitans* was grown as lawns on tryptic soy agar + 0.5% (wt/vol) yeast extract (TSBYE agar medium) under aerobic (5% CO₂ atmosphere) conditions. *S. gordonii* was grown in filter-sterilized TSBYE liquid medium under aerobic conditions without shaking.

Creation of *A. actinomycetemcomitans* transposon library. Plasmid pMR361-K was used to create the *A. actinomycetemcomitans* transposon library. Plasmid pMR361-K was created by first digesting the plasmid pMRKO (ref. 26) with Sall and NotI to excise *mCherry*. Then, the *mariner* transposase C9 gene from pZXL5 (ref. 30) was PCR-amplified with primers Tnp-F-Sall and Tnp-R-NotI (Supplementary Table 3). These primers include Sall and NotI restriction sites at the 5' ends, respectively. The transposase amplicon was then digested with Sall and NotI and ligated into the Sall/NotI-digested pMRKO fragment with *mCherry* removed. These steps replaced *mCherry* with the transposase now positioned downstream of the *lac* promoter. This intermediate vector was then transformed into *Escherichia coli* DH5a, purified and digested with NotI. Next, the kanamycin resistance (KanR) cassette from pCGL0243 (ref. 31) was PCR-amplified with primers KanR-UP-F and KanR-DN-R (Supplementary Table 3). These primers included flanking sequences that base pair with the up- and downstream fragments of the *mariner* inverted repeats. The upstream fragment was PCR-amplified from pZXL5 with primers mar-IR-NotI and mar-UP-R, and the downstream fragment was amplified from pZXL5 with primers mar-DN-F and mar-IR-NotI (Supplementary Table 3). These fragments were then assembled on each end of the KanR cassette by overlap extension PCR, digested with NotI, and ligated into the NotI-digested intermediate vector, generating pMR361-K. pMR361-K was then transformed into *E. coli* DH5a and purified to check the *mariner* inverted repeats by Sanger sequencing. Finally, pMR361-K was moved into the conjugative *E. coli* strain MFDpir (ref. 32). A transposon mutant pool in *A. actinomycetemcomitans* 624 was generated as described in ref. 33 by conjugation with *E. coli* MFDpir (a diaminopimelate auxotroph)³² containing pMR361-K. Conjugations were performed under aerobic and anaerobic conditions on TSBYE agar + 0.3 mM diaminopimelate and pooled before counter-selection under aerobic and anaerobic conditions on TSBYE agar + 40 µg ml⁻¹ kanamycin. Anaerobic conditions were maintained in a vinyl chamber (Coy Lab Products) with the following atmosphere: 85% N₂, 10% CO₂ and 5% H₂. Independent conjugations were combined then aliquoted to generate the final mutant pool.

Murine chronic surgical wound infection. Murine chronic surgical wound infections were performed with six- to eight-week-old female Swiss Webster mice, as previously described^{6,34}. For Tn-seq experiments, 4 × 10⁵ colony-forming unit (c.f.u.) of the *S. aureus* HG003 transposon library were used for mono-infection (*n* = 4 mice) and 2 × 10⁵ *S. aureus* and 2 × 10⁴ *P. aeruginosa* for co-infection (*n* = 3 mice). Wound tissue was collected 4 days post-infection and stored in RNAlater (Ambion). No blinding was used in any of the chronic surgical wound animal experiments, and animals were not randomized. At least three biological replicates were used per condition in this model, which was determined from previous^{6,34} and preliminary data to be sufficient to yield statistically significant differences.

Murine abscess infection. Murine abscess infections with the *A. actinomycetemcomitans* transposon mutant pool were performed with nine- to

eleven-week-old female Swiss Webster mice, as described in refs 26 and 27 with minor modifications. No blinding was used in these experiments, and sample size was determined from previous Tn-seq experiments in this model²⁷ to be sufficient to yield statistically significant differences. Briefly, an aliquot of the mutant pool was grown overnight as lawns under aerobic and anaerobic conditions. The lawns were then pooled in PBS (pH 7.4), adjusted to an optical density at 600 nm (OD₆₀₀) of 2, and mixed with an equal amount of either wild-type *A. actinomycetemcomitans* (for mono-infection inoculum) or *S. gordonii* (for co-infection inoculum). For each mono-infected abscess, 100 µl containing ~1 × 10⁸ of the *A. actinomycetemcomitans* mutant pool and ~1 × 10⁸ of wild-type *A. actinomycetemcomitans* was used (*n* = 2 mice, with two abscesses per mouse). For each co-infected abscess, 100 µl containing ~1 × 10⁸ of the *A. actinomycetemcomitans* mutant pool and ~1 × 10⁸ of *S. gordonii* was used (*n* = 2 mice, with two abscesses per mouse). At 3 days post-infection, each abscess was collected, suspended in 0.9 ml PBS (pH 7.4) in BeadBug tubes pre-filled with 2.8 mm steel beads (Sigma) and homogenized for 30 s in a Mini-Beadbeater (Biospec). A 500 µl volume of each homogenate was then grown in 4.5 ml of TSBYE + 40 µg ml⁻¹ kanamycin for 6 h under aerobic conditions without shaking, before being frozen and stored until preparation for sequencing. The left thigh abscess of each mouse was used for Tn-seq library preparation.

Preparation of *S. aureus* Tn-seq libraries. Sequencing data for the *S. aureus* murine abscess and osteomyelitis models were generated previously^{7,8}. DNA from murine chronic surgical wounds stored in RNAlater was extracted by bead beating, as previously described^{6,35}, with the exception that wound tissue was resuspended in Goodman buffer A + 0.1% SDS + 0.1% sodium deoxycholate. Extracted wound DNA was size-selected for fragments between 100 and 700 bp with Agencourt AMPure XP beads (Beckman Coulter) and prepared for Tn-seq analysis as previously described^{6,35}. Cytidine tails were added with terminal deoxynucleotidyltransferase (TdT), followed by two PCRs. Primers olj376 (ref. 36) and the transposon-specific 5'-biotinylated primer PCR1-Ba-Bio were used for the first PCR for *S. aureus* Tn-seq. An Illumina barcoded primer³ and the transposon-specific primer PCR2-Ba were used for the second PCR for *S. aureus* Tn-seq. The libraries were sequenced at the Genome Sequencing and Analysis Facility at the University of Texas at Austin on an Illumina NextSeq 500 using a 75 bp single-end run.

Preparation of *A. actinomycetemcomitans* Tn-seq libraries. DNA from abscess outgrowths was extracted by vortexing for 1 min with an equal volume of phenol:chloroform:isoamyl alcohol (25:24:1, pH 8) and then purified, beginning at the isopropanol precipitation step², as previously described. Extracted DNA from abscess outgrowths was prepared for Tn-seq analysis as previously described^{6,27}. Cytidine tails were added with terminal deoxynucleotidyltransferase (TdT), followed by two PCRs. Primers olj376 (ref. 36) and the transposon-specific 5'-biotinylated primer mariner-1 were used for the first PCR²⁷ for *A. actinomycetemcomitans* Tn-seq. An Illumina barcoded primer³ and the transposon-specific primer mariner-2 were used for the second PCR²⁷ for *A. actinomycetemcomitans* Tn-seq. The libraries were sequenced at the Genome Sequencing and Analysis Facility at The University of Texas at Austin on an Illumina NextSeq 500 using a 75 bp single-end run.

Essential gene analysis. Reads were trimmed of adapter sequences and mapped to the reference genomes (strain NCTC8325 for *S. aureus* and strain 624 for *A. actinomycetemcomitans*) using the TnSeq2.sh script (available at <https://github.com/spleonard1/Tn-seq>) with bowtie2 v.2.2.5. To minimize the effect of insertions that may not abolish gene function, modified open reading frame assignments were generated for each genome where the 3' 10% of every gene was removed. The following minor modifications were made to the TnSeq2.sh script for *A. actinomycetemcomitans* Tn-Seq analysis: (1) cutadapt (v.1.12)³⁷ was used to trim reads of 3' low-quality bases and 3' poly(C) tail sequences, and to remove reads less than 20 bases long; (2) after mapping, reads that were filtered for high mapping quality (MAPQ > 39) were used to determine the abundance of unique insertion sites while accounting for the 2 bp duplication associated with *mariner* insertion events; and (3) to correct for DNA polymerase slippage²⁸, the read counts of adjacent sites were collapsed onto the site with the highest count (the local maximum) using a custom Python script (available upon request).

The *S. aureus* and *A. actinomycetemcomitans* essential genomes were determined using the following custom scripts with DESeq2 v.1.10.1: TnSeqEssential.sh, TnGeneBin.pl and TnSeqDESeq2Essential.R (available at <https://github.com/spleonard1/Tn-seq>), as previously described^{3,15}. Briefly, the mapped reads were tallied by insertion site, and the 50 most abundant insertion sites were removed to correct for bias resulting from PCR amplification. Only sites that were identified in at least two replicates were considered for downstream analysis. Insertion read counts were smoothed locally by weighted LOESS regression to correct for genomic position-dependent effects on perceived mutant abundance¹⁶. The data were normalized for differences in sequencing depth with estimateSizeFactors() in DESeq2 (ref. 38) and the number of unique insertions and their associated read counts were tallied per gene using the modified open reading frame assignments. Next, 400 pseudodatasets (‘expected data’) were generated, where for each Tn-seq data set, the unique insertions and their associated reads were

randomly redistributed among the 'TA' dinucleotide sites present in the reference genomes (see Supplementary Tables 5 and 6 for a list of the TA sites in the *S. aureus* and *A. actinomycetemcomitans* reference genomes, respectively). Differential mutant abundance between the observed data and the 'expected' pseudodatasets was calculated with a negative binomial test using DESeq2 (ref. 38), with the normalization factors set to one (because normalization had already been performed based on the insertions), with Cook's distance cutoff for outlier removal turned off and with the *P* values adjusted for multiple testing using the Benjamini–Hochberg method³⁸. A parameterized bimodal Gaussian mixture model was fit to the log₂-transformed fold changes in mutant abundance to determine whether a gene was 'reduced' or 'unchanged' using the mclust³⁹ package in R. Genes were called 'essential' if they (1) had a reduced fold change compared to the expected data set (Benjamini–Hochberg adjusted *P* < 0.01, negative binomial Wald test in DESeq2³⁸) and (2) clustered with the lower mode in the characteristic¹⁷ bimodal distribution of fold changes comparing the observed and 'expected' data sets (mclust³⁹ *P* < 0.01). To assess the false positive rate, we used this analysis method to randomly generate data sets from the input library reads that contained the same number of replicates, number of reads and number of insertion sites as the actual data for each condition and to determine the number of falsely identified 'essential genes' using these fitness neutral data. Venn diagrams were generated using Venny (v.2.1)⁴⁰.

Clustering analysis. Read counts for each condition were binned by gene and then used to perform PCA in R. Differences in sequencing depth between each replicate were normalized using the estimateSizeFactors() function and transformed using the rlog function in DESeq2 (v.1.10.1) before analysis. Principal components were then generated from these data using the R prcomp function, and principal component 1 (PC1) and principal component 2 (PC2) were plotted using GraphPad Prism 6. Clustering analysis of the PCA plot was performed in R using k-means in the stats package (v.3.2.2). For hierarchical clustering, Euclidean distances were calculated from the average normalized read counts for each condition before determining clusters using the Ward method in hclust in the stats package (v.3.2.2).

Comparison of mutant fitness in the in vivo chronic surgical wound model. *S. aureus* transposon mutants were constructed by phage transduction (described in section 'Bacterial strains and culture conditions') in the HG003 background from the *S. aureus* JE2 Nebraska Transposon Mutant Library homologues (listed in Supplementary Table 6). For *in vivo* competition experiments, *S. aureus* wild-type strain HG003 or the *S. aureus* HG003 transposon mutants were grown overnight, normalized to an OD₆₀₀ reading of 1.0 in PBS (pH 7.4) and mixed at a ratio of 1:1 mutant to wild type. Mice (*n* = 3 per condition) were inoculated at 7 × 10⁵ for mono-infection and for co-infection at 5 × 10⁵ *S. aureus* and 5 × 10⁵ *P. aeruginosa* PAO1. Wound tissue and the associated bandage were collected (~200–400 mg per wound) 4 days post-infection and added to 0.9 ml PBS (pH 7.4) in BeadBug tubes pre-filled with 2.8 mm steel beads (Sigma) and homogenized for 1 min in a Mini-Beadbeater (Biospec). The homogenate was serially diluted in PBS and plated on BHI agar (to quantify all *S. aureus*) and BHI agar + 10 µg ml⁻¹ erythromycin (to quantify *S. aureus* mutant numbers). *S. aureus* colonies were enumerated and competitive indices for each mutant in each condition were calculated as (no. mutant *S. aureus* c.f.u./g/no. wild-type *S. aureus* c.f.u./g). For co-culture experiments, both *S. aureus* and *P. aeruginosa* formed colonies on BHI but were easily distinguished by colony colour and morphology (small, circular, smooth, yellow colonies for *S. aureus*).

For small-scale Tn-seq experiments using seven mutants, overnight cultures of the *S. aureus* HG003 transposon mutants were normalized to an OD₆₀₀ reading of 1.0 in PBS (pH 7.4) and mixed in equal proportions. An inoculum consisting of 3 × 10⁵ of the *S. aureus* mixture was used for mono-infection (*n* = 3 mice) and co-infection consisted of 1 × 10⁵ *S. aureus* and 6 × 10⁵ PAO1 (*n* = 3 mice). Wound tissue was collected (~100–300 mg of tissue per wound) 4 days post-infection and added to 0.9 ml PBS (pH 7.4) in BeadBug tubes pre-filled with 2.8 mm steel beads (Sigma) and homogenized three times for 1 min in a Mini-Beadbeater (Biospec). A 500 µl volume of the homogenate was added to 4.5 ml of BHI broth containing 10 µg ml⁻¹ erythromycin, and cells were outgrown for 2 h before preparation of DNA for semi-quantitative PCR. Cells were pelleted by centrifugation at 10,000g and resuspended in 200 mM Tris (pH 8.0). LysoStaphin (Sigma) was added at 1 mg ml⁻¹ and *S. aureus* cells were lysed for 1 h at 37 °C. An equal volume of phenol:chloroform:isoamyl alcohol (25:24:1, pH 8) was added and samples were vortexed for 30 s before centrifugation. DNA was purified from the aqueous phase by ethanol precipitation and resuspended in 50 µl H₂O. DNA concentrations were quantified using a NanoDrop, and samples were adjusted to 5 ng µl⁻¹. Semi-quantitative PCRs (see Supplementary Table 3 for primer sequences) were performed using Phusion high-fidelity DNA polymerase (NEB) according to the manufacturer's recommendations for 35 cycles. Densitometry measurements were performed using ImageJ FIJI software (v.2.0.0)⁴¹; the average of ten background measurements was subtracted from each gel, and bands were normalized to PCRs from the *S. aureus* mutant SAOUHSC_00814 (*vWbp*, secreted von Willebrand factor-binding protein) that did not display a fitness defect in mono- or co-infection.

Comparison of mutant fitness in the in vitro Lubbock chronic wound model. Wound-like medium was prepared as previously described²³, and a 600 µl volume was added to tubes (glass, 6 × 50 mm). For mono-culture experiments, wound-like medium

was inoculated with individual transposon mutants (construction as described in section 'Bacterial strains and culture conditions') or the *S. aureus* wild-type strain HG003 at 5 × 10⁴ *S. aureus*. For co-culture experiments, wound-like medium was inoculated with 2.5 × 10⁴ c.f.u. of the *S. aureus* wild type or individual *S. aureus* transposon mutants and 2.5 × 10⁴ c.f.u. *P. aeruginosa* PAO1. Cultures were incubated statically at 37 °C for 6 days and 10 µl samples were removed for bacterial counts on days 2, 4 and 6. *S. aureus* cells were enumerated by plate counts on mannitol salt phenol red agar (Sigma), as this medium does not permit growth of *P. aeruginosa*.

Data availability. The raw sequencing files that support this study have been deposited at the NCBI Sequence Read Archive under accession no. SRP093229 for *S. aureus* Tn-seq data and accession no. SRP095181 for *A. actinomycetemcomitans* Tn-seq data. The sequenced genome for *S. aureus* reference strain NCTC8325 is available under RefSeq accession no. NC_007795.1. The sequenced genome for *A. actinomycetemcomitans* Strain 624 is available under RefSeq accession no. NZ_CP012959.1. The sequence for plasmid pMR361-K is available under GenBank accession no. KY767032. The remaining data that support the findings of this study are available from the corresponding author upon request.

Received 11 April 2016; accepted 14 April 2017;
published 30 May 2017

References

- Lewis, K. *Nat. Rev. Drug Discov.* **12**, 371–387 (2013).
- Le Breton, Y. *et al. Sci. Rep.* **5**, 9838 (2015).
- Turner, K. H., Wessel, A. K., Palmer, G. C., Murray, J. L. & Whiteley, M. *Proc. Natl Acad. Sci. USA* **112**, 4110–4115 (2015).
- Umland, T. C. *et al. mBio* **3**, e00113-12 (2012).
- van Opijnen, T. & Camilli, A. *Nat. Rev. Microbiol.* **11**, 435–442 (2013).
- Turner, K. H. *et al. PLoS Genet.* **10**, e1004518 (2014).
- Valentino, M. D. *et al. mBio* **5**, e01729-14 (2014).
- Wilde, A. D. *et al. PLoS Pathog.* **11**, e1005341 (2015).
- Stacy, A., McNally, L., Darch, S. E., Brown, S. P. & Whiteley, M. *Nat. Rev. Microbiol.* **14**, 93–105 (2015).
- Chambers, H. F. & Deleo, F. R. *Nat. Rev. Microbiol.* **7**, 629–641 (2009).
- Lowy, F. D. *N. Engl. J. Med.* **339**, 520–532 (1998).
- Cheng, A. G., DeDent, A. C., Schneewind, O. & Missiakas, D. *Trends Microbiol.* **19**, 225–232 (2011).
- Gjodsbøl, K. *et al. Int. Wound J.* **3**, 225–231 (2006).
- Madsen, S. M., Westh, H., Danielsen, L. & Rosdahl, V. T. *APMIS* **104**, 895–899 (1996).
- Powell, J. E., Leonard, S. P., Kwong, W. K., Engel, P. & Moran, N. A. *Proc. Natl Acad. Sci. USA* **113**, 13887–13892 (2016).
- Zomer, A., Burghout, P., Bootsma, H. J., Hermans, P. W. & van Hijum, S. A. *PLoS ONE* **7**, e43012 (2012).
- Dalton, T. *et al. PLoS ONE* **6**, e27317 (2011).
- Korgaonkar, A., Trivedi U., Rumbaugh K. P. & Whiteley M. *Proc. Natl Acad. Sci. USA* **110**, 1059–1064 (2013).
- Fazli, M. *et al. J. Clin. Microbiol.* **47**, 4084–4089 (2009).
- Gottrup, F. *Wound Repair Regen.* **12**, 129–133 (2004).
- Anderson, M., Chen, Y. H., Butler, E. K. & Missiakas, D. M. *J. Bacteriol.* **193**, 1583–1589 (2011).
- Cao, Z., Casabona, M. G., Kneuper, H., Chalmers, J. D. & Palmer, T. *Nat. Microbiol.* **2**, 16183 (2016).
- Sun, Y., Dowd, S. E., Smith, E., Rhoads, D. D. & Wolcott, R. D. *Wound Repair Regen.* **16**, 805–813 (2008).
- DeLeon, S. *et al. Infect. Immun.* **82**, 4718–4728 (2014).
- Welch, M. J. L., Rossetti, B. J., Rieken, C. W., Dewhirst, F. E. & Borisy, G. G. *Proc. Natl Acad. Sci. USA* **113**, E791–E800 (2016).
- Ramsey, M. M., Rumbaugh, K. P., Whiteley, M. & Sullam, P. M. *PLoS Pathog.* **7**, e1002012 (2011).
- Stacy, A., Fleming, D., Lamont, R. J., Rumbaugh, K. P. & Whiteley, M. *mBio* **7**, e00782-16 (2016).
- Gallagher, L. A., Shendure, J. & Manoil, C. *mBio* **2**, e00315-10 (2011).
- Olson, M. E. in *The Genetic Manipulation of Staphylococci* 69–74 (Springer, 2015).
- Zhang, X. *et al. PLoS Genet.* **8**, e1002804 (2012).
- Reyes, O. *et al. Gene* **107**, 61–68 (1991).
- Ferrieres, L. *et al. J. Bacteriol.* **192**, 6418–6427 (2010).
- Mintz, K. P. *Microbiology* **150**, 2677–2688 (2004).
- Watters, C. *et al. Med. Microbiol. Immunol.* **202**, 131–141 (2013).
- Murray, J. L., Kwon, T., Marcotte, E. M. & Whiteley, M. *mBio* **6**, e01603-15 (2015).
- Klein, B. A. *et al. BMC Genomics* **13**, 578 (2012).
- Martin, M. *EMBnet* **17**, 10–12 (2011).
- Love, M. I., Huber, W. & Anders, S. *Genome Biol.* **15**, 550 (2014).
- Fraley, C. & Raftery, A. E. *J. Am. Stat. Assoc.* **97**, 611–631 (2002).

40. Oliveros, J. C. VENNY. An interactive tool for comparing lists with Venn's diagrams (*BioinfoGP*, 2007–2015); <http://bioinfogp.cnb.csic.es/tools/venny/index.html>
41. Schindelin, J. *et al. Nat. Methods* **9**, 676–682 (2012).

Acknowledgements

This work was supported by the National Institutes of Health (NIH, grants R01GM116547-01A1 and 1R01DE023193-01 to M.W.) and a grant from Human Frontiers Science (to M.W.). C.B.I. is supported by postdoctoral fellowship IBBERS16F0 from the Cystic Fibrosis Foundation. Contributions by M.S.G. were supported by PHS grant AI107248 and the Harvard-wide Program on Antibiotic Resistance (AI083214). A.S. is supported by a predoctoral fellowship from the NIH (F31DE024931). The authors thank M. Ramsey for generating pMR361-K, K. Michie for assistance with the chronic surgical wound experiments, S. Leonard for computational assistance and D. Cornforth for discussion of the manuscript.

Author contributions

C.B.I., A.S., K.R. and M.W. designed experiments. C.B.I., A.S. and M.W. analysed data. C.B.I., A.S. and D.F. performed experiments. J.L.D. prepared sequencing libraries.

M.S.G. provided *S. aureus* HG003 transposon library and provided the raw data from previous studies^{7,8} included in the analysis. C.B.I., A.S., J.L.D., M.S.G., K.R. and M.W. wrote the paper.

Additional information

Supplementary information is available for this paper.

Reprints and permissions information is available at www.nature.com/reprints.

Correspondence and requests for materials should be addressed to M.W.

How to cite this article: Ibberson, C. B. *et al.* Co-infecting microorganisms dramatically alter pathogen gene essentiality during polymicrobial infection. *Nat. Microbiol.* **2**, 17079 (2017).

Publisher's note: Springer Nature remains neutral with regard to jurisdictional claims in published maps and institutional affiliations.

Competing interests

The authors declare no competing financial interests.